

리튬이차전지 음극재 성능에 미치는 수계 바인더 점도 영향 연구

강현철[#] · 신은선[#] · 황기범 · 김재광 · 윤성훈[†]

중앙대학교 융합공학부

(2021년 12월 24일 접수, 2022년 2월 3일 수정, 2022년 2월 4일 채택)

Influence of Aqueous Carboxymethyl Cellulose Binder Viscosity on the Anode Performance in Lithium Ion Batteries

Hyunchul Kang[#], Eunsun Shin[#], Keebum Hwang, Jaekwang Kim, and Songhun Yoon[†]

Department of Integrative Engineering, Chung-Ang University, Seoul 06974, Korea

(Received December 24, 2021; Revised February 3, 2022; Accepted February 4, 2022)

초록: 리튬이차전지 수계 바인더인 carboxymethyl cellulose (CMC)의 점도가 흑연과 바인더, 그리고 집전체에 접착력에 변화시켜 음극재의 전기화학 성능에 미치는 영향을 조사하였다. 분자량이 다른 세 종류의 CMC 바인더를 이용하여, 바인더의 수계 분산 상태와 흑연음극재에 첨가된 슬러리 용액의 점도 특성을 레오미터를 이용하여 분석하였다. 이러한 유변학적 특성 변화는 흑연과 바인더와의 결합력에 의존한다는 것을 알 수 있었다. 세 종류의 바인더를 리튬이차전지 음극재에 적용한 결과, 점도가 가장 높은 CMC 바인더에서 가장 우수한 음극 성능(140사이클 후 88.0%, 220.6 mA h g⁻¹ @ 2C rate)을 얻을 수 있었으며 이는 높은 집전체와의 결합력에 기인함을 알 수 있었다. 또한 다양한 미세구조 형성에 따라 음극의 사이클 성능개선과 낮은 속도 특성이 발현됨을 확인하였다(140사이클 후 86.3%). 이를 통해 슬러리 용액의 유변학적 특성이 흑연 음극의 전기화학적 특성에 큰 영향을 미칠 수 있음을 알 수 있었다.

Abstract: Viscosity effect of carboxymethyl cellulose (CMC), an aqueous binder for lithium secondary batteries, on the electrochemical performance of graphite anode materials is investigated by changing the adhesion to graphite, binder, and current collector. Using three CMC binders with different molecular weight, viscosity of pure aqueous solutions and anode slurry solutions with graphite materials are compared using rheometer. The rheological trend is dependent on the interaction between CMC binder and graphite material. After fabrication of the anodes in lithium ion batteries, the binder with highest viscosity showed the best cycle and rate performances; 88.0% @ 140 cycles and 220.6 mA h g⁻¹ @ 2C rate, which is attributed to high adhesion strength with current collector. Furthermore, formation of different microstructures results in advanced cycle performance and low rate capability (86.3% after 140 cycles) from the enhanced viscosity slurry solution in spite of weak adhesion property with current collector. Hence, the rheology of the slurry solution can critically influence on the electrochemical performance of the graphite anode in LIBs.

Keywords: carboxymethyl cellulose, aqueous binder, rheology, graphite anode, lithium-ion batteries.

Introduction

Since the first production of the commercial lithium-ion battery (LIB) in the 1990s, extensive research efforts have been tried for the improvement of LIB performance. Research into LIBs has focused on two areas: electrode material synthesis and electrochemistry. Typical negative electrodes

are composed of a carbonaceous active material, a conductive additive, and a binder. During the electrode fabrication process, three materials are typically blended with a solvent, followed by coating onto the current collector and drying.¹⁻⁴ Carbonaceous materials such as soft carbon, hard carbon, and graphite have been utilized as the main active material in anodes because of their high capacity, performance, and stability and wide-scale availability. To improve the performance of carbon-based anodes, electrode fabrication and the selection of components such as a conducting agent and binder must be optimized. The binders play particularly

[#]These authors are equally contributed to this work.

[†]To whom correspondence should be addressed.

yoonsun@cau.ac.kr, ORCID[®] 0000-0002-0962-7470

©2022 The Polymer Society of Korea. All rights reserved.

important roles for establishing strong adhesion of electrode active materials and for maintaining the mechanical stability of active anode layers on the current collector. Previously, the N-methyl-2-pyrrolidone (NMP)-soluble binder was based on a fluoride polymer. More recently, however, cellulose-based binders, such as carboxymethyl cellulose (CMC), which are dispersed in an aqueous solvent, have been employed due to their high environmental safety, wide availability, and inexpensiveness.⁵⁻⁷ The anode slurry is typically an inhomogeneous mixed phase that comprises graphite or carbon black as a particle, CMC as a binder, and an aqueous medium as a solvent. Multiple microstructures can be organized because of the interaction between the particle and the polymer such as through bridging, depletion attraction, or electrostatic repulsion.⁸ It has been noted that the microstructure in the slurry is dependent on the ratio of between CMC binder and graphite. If the ratio of CMC to graphite is low, graphite particles are dispersed in the slurry because of steric repulsion by adsorbed CMC on graphite. When the ratio of CMC to graphite is high, however, the aggregation of graphite particles occurs because of depleted attraction by non-adsorbed CMC. In this way, films having different microstructures can be prepared according to the change in the microstructure of the slurry, which has a strong influence on anode performance. It has been reported that the polymeric binder affects particle dispersion in the anode slurry, dried film characteristics, and battery performance.⁹⁻¹² Lee *et al.* investigated the microstructures of the slurry and the electrode as a result of the mixing protocol, and determined that high dispersion of the slurry results in LIB performance improvement. This reflects that determination of the main factors is important in affecting microstructure formation of the slurry to enhance battery performance; these factors are significant because graphite particles tend to become aggregated in an aqueous solvent because of the presence of non-polar surfaces and hydrophobicity, indicating the significance of their dispersion in an aqueous solution. In addition, the effect of CMC on the dispersion of graphite particles and on the viscosity of the slurry in the aqueous solution, should be investigated.¹³⁻¹⁸ However, there is a shortage of research into the origin of viscosity induced by the binders in the aqueous anode slurry.

Herein, the effect of CMC on viscosity can be investigated by employing three types of CMC binders. Using rheological measurements, the viscosity of an aqueous solution containing only three CMC binders and that of the mixed slurry with

graphite active materials were analyzed. In addition, slurry conditions such as stirring time and speed were varied to allow for direct comparison of the graphite morphology and electrical and mechanical properties. After fabrication of the anodes, the electrochemical behavior of half cells using three binders was studied.

Experimental

Electrode Preparation. The CMC binder was obtained by GLCHEM. Natural graphite from POSCO CHEMICAL was used as an active material and carbon black (CB) (Super P) (KETI, Korea) as a conductive additive. The electrode composition was determined at 90/5/5 wt% (graphite/CB/binder). A copper foil (20 μm thick, KETI, Korea) as the current collector was utilized. Three types of CMC binders (DS=0.8-1.2, CMC1 $M_w=978172$, CMC2 $M_w=748148$, CMC3 $M_w=612426$, GLCHEM) were employed as a binder for comparison. Graphite (KETI, Korea), CB and CMC binder were mixed in an agate mortar for 1 hour after dropwise addition of D.I water into the slurry mixture for 5 min. After mixing, styrene-butadiene-rubber (SBR) (KETI, Korea) was added for 5 min, which formed a homogenized ink. This ink was coated onto the Cu current collector using a doctor-blade technique. Here, battery grade SBR from MTI corporation (butadiene 70-72%, styrene 23-25%) was utilized as co-additive binder. After drying electrodes at 80 $^{\circ}\text{C}$ for 12 h in a vacuum oven, they were stored in an argon-filled glove box and used as anodes in lithium ion batteries.

Electrochemical Performance. Conventional CR2032 two-electrode coin cells were fabricated for anode performance test. They were assembled in a glove box using coin-cell components (1.2 cm diameter from Welcos, Japan), electrolyte reservoir, separator, and a lithium metal disk (MTI, 1.8 cm diam.), which used as a counter electrode. A 1 M LiPF_6 in a 3/7 volume ratio mixture of Brookfield, ethylene carbonate/ethyl methyl carbonate (EC/EMC) (KETI, Korea) was utilized as electrolyte. Using a WonaTECH cycler, galvanostatic charge-discharge experiments were conducted. Cycling condition was voltage cut-off between 3.0 and 4.3 V vs. Li/Li^+ and C-rates ranging from C/10 to 20 C. 1 C-rate current condition was calculated using the theoretical capacity of graphite (372 mA h g^{-1}).

Rheological Measurements. The rheology of different aqueous solutions containing only CMC binders were evaluated

at 25 °C on a controlled-stress rotating rheometer (DV-II+Pro, Brookfield, Canada) with a 3 cm diameter plane-plane geometry under several speeds. Also, other measurement were obtained with continuous shear. Sweep rate was ranged from 0.1 to 1000 s⁻¹, which was conducted both with and without graphite/CB. In order to investigate the rheology of the electrode slurry, the DV-II+Pro apparatus was utilized.

Peeling Strength Test. The peeling strength between the copper foil and the electrode was measured using tensile test machine (JSV-H1000, JISC, Korea). An adhesive tape (3 M, 10 cm width) was bonded by pressing it onto the electrode strip, which was fixed on a glass plate by using a double-faced adhesive tape. After a period of relaxation time, peeling test at an angle of 180° was conducted under a speed of 10 mm min⁻¹. The relationship between tensile force and the peeling displacement were measured.

Results and Discussion

Figure 1 shows the dependence of the viscosity on shear rate for the aqueous solutions of the three CMC materials and electrode slurries mixed with graphite and carbon black. This figure reveals the solution behavior and the influence of graphite on the rheological properties of the slurries, indicative of the typical shear thinning behavior related with a typical decrease in the viscosity at increasing shear rate. Flow curves of pure aqueous CMC solutions demonstrate a clear shear thinning behavior within the shear rate range from 10⁻¹ to 10³ s⁻¹. According to the decrease in initial viscosity in the three CMC binders, the shear thinning effect became less obvious, and the final viscosity at a shear rate of 100 s⁻¹ is alike for all three binders, as listed in Table 1. When applied to the electrode slurry solution, the trend in initial viscosity is different from that observed

for the pure aqueous binder solutions, suggesting that slurry viscosity is highly relevant to the added binder. During slurry preparation, the graphite particles typically form a gel structure via hydrophobic attraction in the aqueous solution. When SBR is added to the slurry solution, it is adsorbed onto graphite and weakens the attractive force among the graphite particles. The graphite particles are scattered by electrostatic repulsion between the CMC molecules. As the initial CMC viscosity is further increased, the slurry displays more gel-like behavior because of the polymeric network structure formed by the CMC molecules. Note that the gel structure can be maintained by the aggregation of graphite particles even at Table 1. Therefore, the rheological phenomena should be observed in order to identify the microstructure formation of graphite-CMC/SBR slurry, which can influence the electrode performance. As seen in Figure 1(b), monotonous decrease in viscosity is observed, which correlates to an increase in shear rate; this result is alike to that observed for the pure aqueous CMC solution. The shear thinning effect is stronger in the CMC3 slurry because the comparison of viscosity data under 6 s⁻¹ shear rate. At high shear stresses, the agglomerates of the slurry containing graphite, carbon black and SBR/CMC binder can be disintegrated because of the increased energy input, which is more obvious in the CMC3 slurry solution. In contrast, the shear thinning is less significant in the CMC1 and CMC2 slurries, indicating that the interaction between CMC and SBR is different than that in the CMC3 case. Furthermore, this rheological behavior can be exploited to determine the optimal mixing conditions for electrode fabrication. Under the initial high viscosity conditions of the CMC binder, electrode mixing is more rapid but mixing time can be extended during the slurry preparation. Hence, we employed initial low mixing speeds as well as the final, high

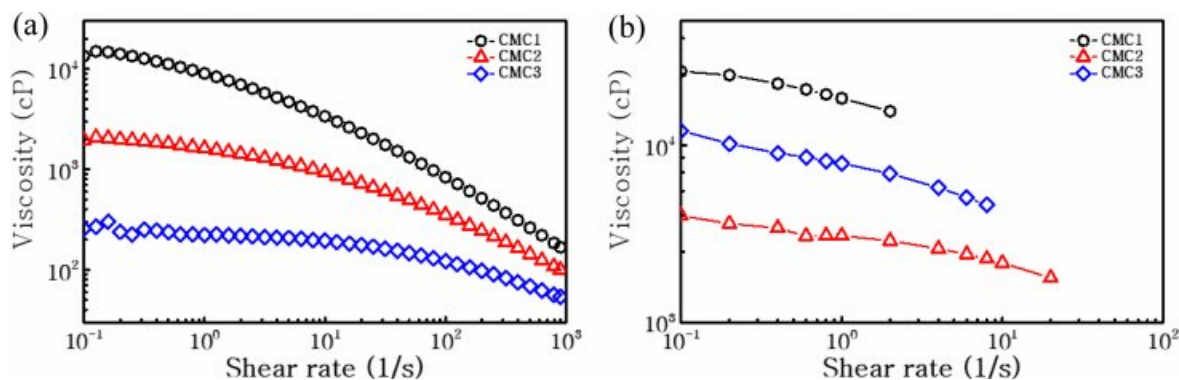
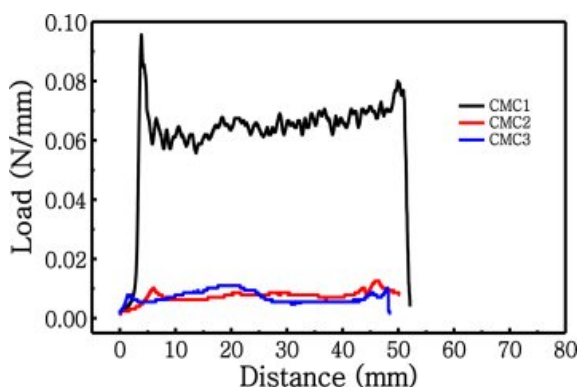


Figure 1. Viscosity versus shear rate for the CMC solution (a) without; (b) with graphite.

Table 1. Viscosity and Shear Rate for CMC Solutions without Graphite

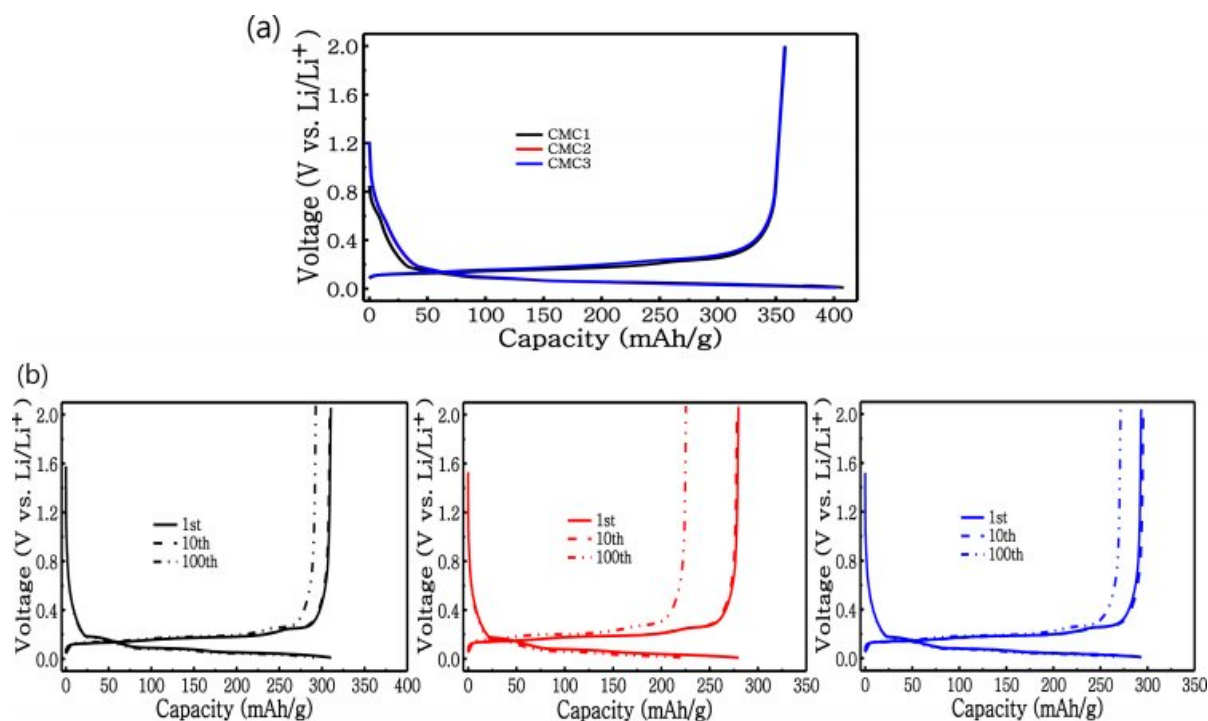
Shear rate (1/S)	CMC1	CMC2	CMC3
1	9042.0	1620.6	221.1
10	3373.7	936.8	194.2
100	837.0	352.9	122.2

**Figure 2.** Adhesion strength profiles of graphite measured by the peeling test.

mixing speeds on the basis of the rheological tendency in Figure 1. After the fabrication of individual electrodes, adhesion strength was analyzed; the results are shown in

Figure 2. As the electrode performance can be affected by adhesion among active particles, carbon additives, and the current collector, weak adhesion among these components can create cracks within the active materials, or cause the detachment of active material layers from the current collector, leading to a decrease in capacity and low cycling stability. Thus, the adhesive properties of the anodes were evaluated through a 180° peeling test; the adhesion strength profiles are shown in Figure 2. These profiles demonstrate that the CMC1 binder displays a high average peeling force of $\sim 0.065 \text{ N mm}^{-1}$ with relatively stable peeling curves. This force is notably higher than those of the two other binders ($\sim 0.007 \text{ N mm}^{-1}$). The results suggest that the CMC1 binder is optimal for the attachment with the current collector. As a result, the initial binder viscosity can be the significant factor in the fabrication of stable composite electrodes.

In order to compare the anode performance of composite electrodes, cycling tests were conducted and results are displayed in Figure 3. In this figure, the coin half-cell test was carried out at a 0.1 C rate between 0 and 2 V vs. Li/Li⁺. Figure 3(a) exhibits the initial charge-discharge patterns for three electrodes. No significant differences are observed in the three anodes, which is in accordance with the data

**Figure 3.** (a) Voltage profile for anodes made from graphite at the viscosity derived from first cycle of 0.1 C; (b) cycling performance at a charging/discharging rate of 1 C.

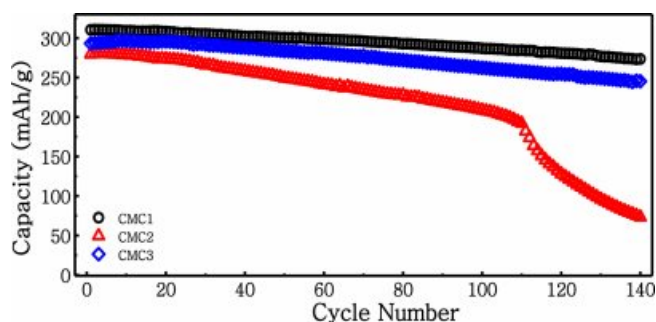


Figure 4. Cycling performance of graphite electrode operated at 1 C for 140 cycles at 25 °C.

shown in Figure 3(a). In order to compare the variation in the charge-discharge patterns during cycling, the 1st, 10th and 100th patterns are compared. Clear capacity fading is observed here; the CMC1 anode displays higher capacity retention even after 100 cycles than the other two electrodes. The capacity loss is up to 10.6% and 25.4%, which correspond to the capacities of 208.6 and 262.2 mA h g⁻¹ for CMC2 and CMC3, respectively. However, the capacity loss for the anode with the CMC1 binder is only 7.6%; the specific discharge capacity was maintained at 287.0 mA h g⁻¹. This highly advanced capacity retention for identical graphite active material reflects the fact that the binder can greatly influence the anode performance because of the strong adhesion between the graphite and the current collector (as shown in Figure 2).

In order to confirm the difference in capacity retention, the cycling performance of the anodes was investigated for up to 140 cycles in Figure 4. Here, a highly stable cycle performance is observed for the CMC1 electrode, which results in a reversible capacity of 273 mA h g⁻¹ after 140 cycles (88.0% capacity retention). In contrast, the CMC2 and CMC3 anodes showed 26.2% and 86.3% capacity retention, respectively. Note that the cycle retention of the CMC3 anode is comparable to that of the CMC1 anode. As shown in the rheological measurement for the electrode slurry in Figure 1(b), CMC3 formed a more viscous slurry even after it had been mixed with graphite and carbon black, which can result in high dispersion among the components of the electrode materials. As mentioned in Figure 1(b), this was probably due to the difference in the interactions of CMC1 and CMC3 with SBR. Therefore, it can be stated that the adhesion property and slurry viscosity can have a significant influence on stable electrode formation.

The discharge curves in Figure 5 shows the rate

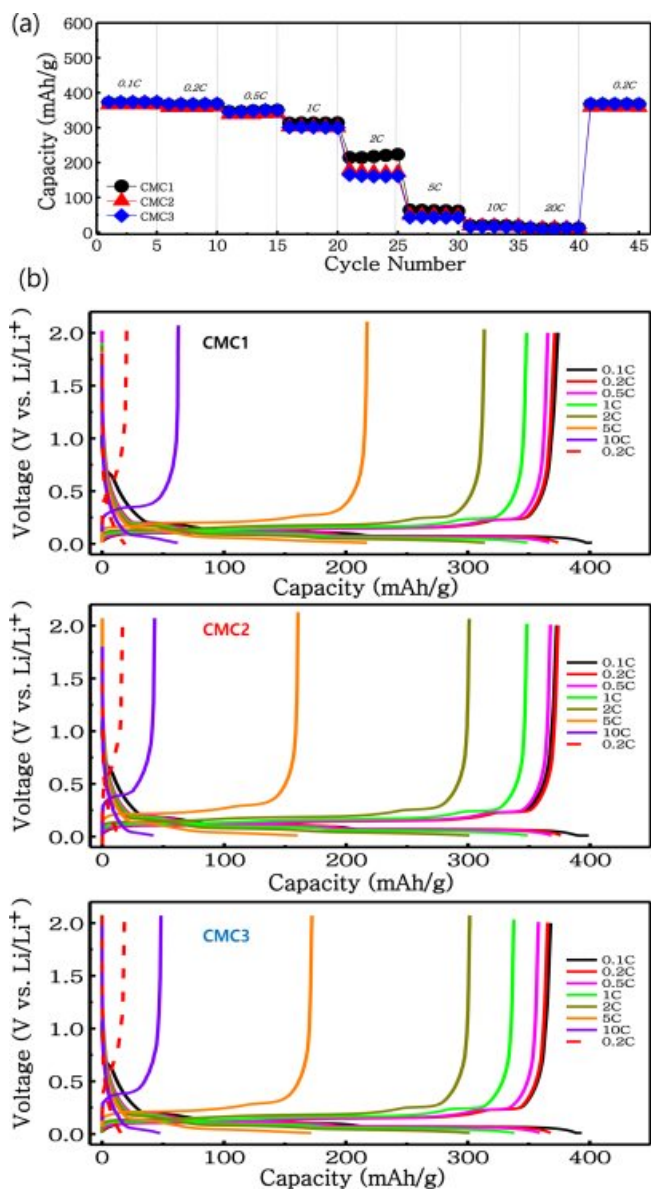


Figure 5. (a) Cycling performance of graphite electrodes at different C rates from 0.1 to 20 C using CMC binders as the viscosity; (b) charge and discharge patterns.

performance and the galvanostatic charge-discharge profiles recorded under various current rates ranging from 0.1 to 20 C. The discharge capacity is dependent upon the discharge rate for the electrodes. When the rate is higher than 10 C, a slight difference exists between the three electrodes because the applied current was very high to facilitate lithium ion intercalation. A clear difference, however, is observed up until the 2 C rate, whereat the CMC1 electrode retains a high capacity of 220.6 mA h g⁻¹, while it retains 64.1 mA h g⁻¹ at 5 C. This indicates that the CMC1 binder has a

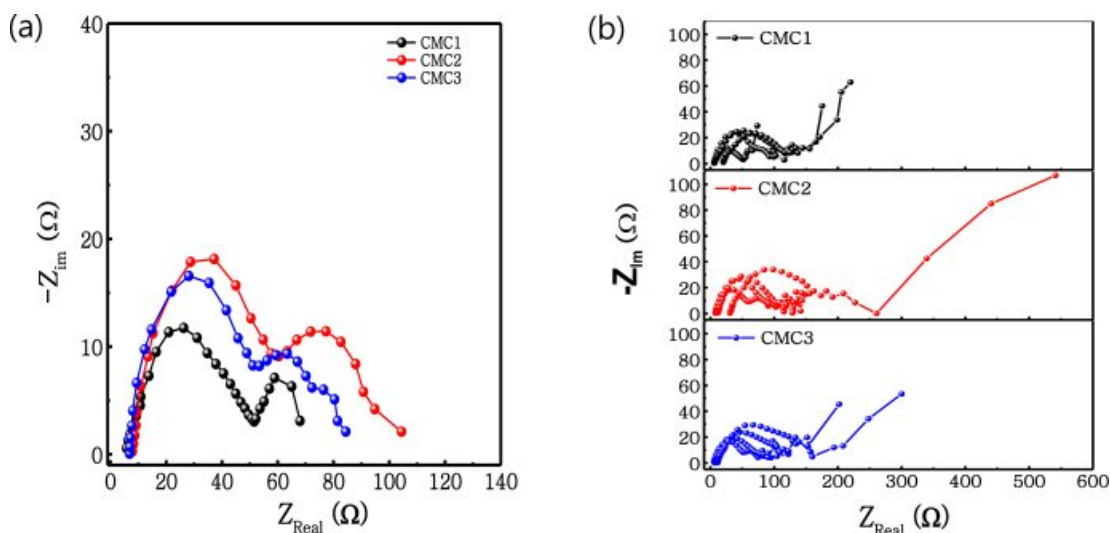


Figure 6. Impedance spectra of unit cells containing graphite electrode after (a) precycling; (b) 1, 10, 100, and 140 cycle.

highly optimized electrode structure because of the well-developed microstructure of the electrode slurry when applied for anode fabrication. This indicates stable cycling performance and good rate capability. In order to determine the difference in rate and cycling performances, an electrochemical impedance spectroscopy (EIS) experiment was carried out for the three anodes. Figure 6(a) shows the Nyquist plots of the three anodes after the first charging. Here, the three anodes exhibit two semicircles in the high-to-middle frequency region, which represent the solid electrolyte interphase (SEI) film (R_f) and the charge transfer resistance (R_{ct}), respectively. The sloped line in the low frequency region is associated with lithium chemical diffusion in the graphite anode. Along this line, the Nyquist plots can be simulated by the equivalent circuit as a Randal circuit (inset of Figure 6). In this equivalent circuit, R_f and C_{sl} are the resistance and capacitance of the SEI film. R_{ct} and C_{dl} represent the charge transfer resistance and double layer capacitance, respectively. The R_f and R_{ct} values for the CMC1 anode after initial charging are 57 and 73 Ω , respectively, both of which are much lower than those of the CMC2 and CMC3 electrodes, *i.e.* 69 and 91 Ω and 74 and 113 Ω , respectively. This reflects that the CMC1 anode showed a low resistance component in both R_f and R_{ct} , which was relevant to the improved rate performance in Figure 5. From Figure 6(b)-(d), the impedance change according with cycling was compared the results in the Nyquist plot. All impedance tests were performed in a full delithiated state after complete discharging at 2 V vs. Li/

Li⁺. It is clearly observed that the resistance values of the three anodes increased with cycling. Importantly, a limited increase in overall impedance spectra is observed for the CMC1 and CMC3 anodes, which reflects that electrode integrity was maintained without a significant exposure of a new SEI layer (stable SEI film). In contrast, the increase in impedance spectra is obvious in the CMC2 electrode. This change of the impedance spectra was highly similar to the cycling behavior shown in Figure 4.

Conclusions

In this study, CMC with various initial viscosities was used as a binder for the fabrication of LIB anodes. The binder with the highest viscosity exhibited the optimal cycle and rate performances after when used for anode fabrication because of high adhesion strength with the current collector. In spite of low viscosity in the pure aqueous CMC solution, however, increased viscosity in the slurry solution was observed, which was attributed to the formation of different microstructures as a result of the change of the interaction with SBR. This anode also exhibited acceptable anode performance despite of its weak adhesion properties. Hence, it was concluded that the rheological phenomena of the slurry solution were the most crucial factor for the electrochemical performance of the graphite in LIBs.

Acknowledgment: This research was supported by the Chung-Ang University Research Scholarship Grants in 2021

(assistant researcher A). Also, this work is supported by the National Research Foundation of Korea (NRF), funded by the Korea government (MSIT) (No.2021-0-01777).

Conflict of Interest: The authors declare that there is no conflict of interest.

References

- Li, J.; Daniel, C.; Wood, D. Materials Processing for Lithium-ion Batteries. *J. Power Sources* **2011**, 196, 2452-2460.
- Jabbour, L.; Bongiovanni, R.; Chaussy, D.; Gerbaldi, C.; Beneventi, D. Cellulose-based Li-ion Batteries: A Review. *Cellulose* **2013**, 20, 1523-1545.
- Scrosati, B.; Garche, J. Lithium Batteries: Status, Prospects and Future. *J. Power Sources* **2010**, 195, 2419-2430.
- Wang, Q.; Ping, P.; Zhao, X.; Chu, G.; Sun, J.; Chen, C. Thermal Runaway Caused Fire and Explosion of Lithium Ion Battery. *J. Power Sources* **2012**, 208, 210-224.
- Ryou, M. H.; Kim, J.; Lee, I.; Kim, S.; Jeong, Y. K.; Hong, S.; Ryu, J. H.; Kim, T. S.; Park, J. K.; Lee, H.; Choi, J. W. Mussel-inspired Adhesive Binders for High-performance Silicon Nanoparticle Anodes in Lithium-ion Batteries. *Adv. Mater.* **2013**, 25, 1571-1576.
- Kovalenko, I.; Zdyrko, B.; Magasinski, A.; Hertzberg, B.; Milicev, Z.; Burtovyy, R.; Luzinov, I.; Yushin, G. A Major Constituent of Brown Algae for Use in High-capacity Li-ion Batteries. *Science* **2011**, 334, 75-79.
- Koo, B.; Kim, H.; Cho, Y.; Lee, K. T.; Choi, N. S.; Cho, J. A Highly Cross-linked Polymeric Binder for High-performance Silicon Negative Electrodes in Lithium Ion Batteries. *Angew. Chem., Int. Ed.* **2012**, 51, 8762-8767.
- Zheng, H.; Tan, L.; Liu, G.; Song, X.; Battaglia, V. S. Calendering Effects on the Physical and Electrochemical Properties of $\text{Li}[\text{Ni}_{1/3}\text{Mn}_{1/3}\text{Co}_{1/3}]\text{O}_2$ Cathode. *J. Power Sources* **2012**, 208, 52-57.
- Tran, H. Y.; Greco, G.; Täubert, C.; Wohlfahrt-Mehrens, M.; Haselrieder, W.; Kwade, A. Influence of Electrode Preparation on the Electrochemical Performance of $\text{LiNi}_{0.8}\text{Co}_{0.15}\text{Al}_{0.05}\text{O}_2$ Composite Electrodes for Lithium-ion Batteries. *J. Power Sources* **2012**, 210, 276-285.
- Lee, G.-W.; Ryu, J. H.; Han, W.; Ahn, K. H.; Oh, S. M. Effect of Slurry Preparation Process on Electrochemical Performances of LiCoO_2 Composite Electrode. *J. Power Sources* **2010**, 195, 6049-6054.
- Lee, J.-H.; Paik, U.; Hackley, V. A.; Choi, Y.-M. Effect of Carboxymethyl Cellulose on Aqueous Processing of Natural Graphite Negative Electrodes and their Electrochemical Performance for Lithium Batteries. *J. Electrochem. Soc.* **2005**, 152, A1763.
- Buqa, H.; Holzapfel, M.; Krumeich, F.; Veit, C.; Novák, P. Study of Styrene Butadiene Rubber and Sodium Methyl Cellulose as Binder for Negative Electrodes in Lithium-ion Batteries. *J. Power Sources* **2006**, 161, 617-622.
- Koos, E.; Willenbacher, N. Capillary Forces in Suspension Rheology. *Science* **2011**, 331, 897-900.
- Koos, E.; Dittmann, J.; Willenbacher, N. Kapillarkräfte in Suspensionen: Rheologische Eigenschaften und potenzielle Anwendungen. *Chem. Ing. Tech.* **2011**, 83, 1305-1309.
- Sorrell, C. A. Liquid Viscosity Measurement Using a Buret. An Instructional Technique. *J. Chem. Educ.* **1971**, 48, 252.
- Urian, R. C.; Khundkar, L. R. A Diode-Laser Based Automated Timing Interface for Rapid Measurement of Liquid Viscosity. *J. Chem. Educ.* **1998**, 75, 1135.
- Doroodmand, M. M.; Maleki, N.; Kazemi, H. A Low-Cost Viscometer from an Opto-Mechanical Mouse. *J. Chem. Educ.* **2010**, 87, 1411-1413.
- Spahr, M. E.; Goers, D.; Leone, A.; Stallone, S.; Grivei, E. Development of Carbon Conductive Additives for Advanced Lithium Ion Batteries. *J. Power Sources* **2011**, 196, 3404-3413.

출판자 공지사항: 한국고분자화학회는 게재된 논문 및 기관 소속의 관할권 주장과 관련하여 중립을 유지합니다.